Electrochemical Observation of Single Collision Events: Fullerene Nanoparticles

Emma J. E. Stuart, Kristina Tschulik, Christopher Batchelor-McAuley, and Richard G. Compton*

Department of Chemistry, Physical & Theoretical Chemistry Laboratory, Oxford University, South Parks Road, Oxford, OX1 3QZ, United Kingdom

ABSTRACT Individual fullerene nanoparticles are detected and sized in a non-aqueous solution *via* cathodic particle coulometry where the direct, quantitative reduction of single nanoparticles is achieved upon collision with a potentiostated gold electrode. This is the first time that the nanoparticle impact technique has been shown to work in a non-aqueous electrolyte and utilized to *coulometrically* size carbonaceous nanoparticles. Contrast is drawn between single-nanoparticle electrochemistry and that seen using nanoparticle ensembles *via* modified electrodes.

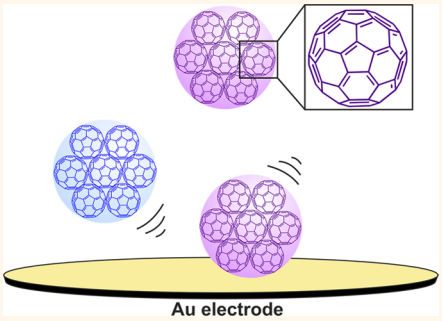

KEYWORDS: fullerene nanoparticles · nano-C_{60} · single-nanoparticle sizing · cathodic particle coulometry · nanoparticle–electrode collision · nanoimpacts

Electrochemical techniques have been invaluable in the investigation of fullerene molecules with the most studied being buckminsterfullerene, C_{60}.[1] C_{60} has been found to undergo both oxidation and reduction.[2] Up to six successive one-electron reductions of C_{60} in solution have been reported under certain conditions.[3] While the electrochemistry of C_{60} molecules, C_{60} molecular films and other colloidal carbon-based materials[4] have been studied in detail, the electrochemical properties of C_{60} nanoparticles (NPs), or nano-C_{60}, remain unexplored.[5,6] The nanoparticulate form of C_{60} has gained increasing attention due to the spontaneous aggregation of C_{60} molecules in environmental waters to form nano-C_{60}.[7] Significant environmental exposure to C_{60} and thus nano-C_{60} formation is likely given the mass production of C_{60} for manifold applications ranging from cosmetics[8] to photovoltaics,[9] while C_{60} has also been found to occur naturally in the environment.[10,11] Reports that nano-C_{60} is bactericidal[12] and toxic to human cell lines[13] have resulted in a need to monitor these carbonaceous nanoparticles.

A method to detect individual NPs has been developed where an electrocatalytic reaction occurs exclusively on NPs in contact with an inert electrode surface, thereby resulting in an amplification of the current response upon NP–electrode collision.[14–19] The detection of single-walled carbon nanotubes (SWCNTs) has been achieved using this non-coulometric NP-impact technique *via* investigation of increasing electrode area and therefore amplified currents for ferrocenemethanol oxidation upon SWCNT collision.[20] One drawback of this electrocatalytic amplification method for NP detection is that the types of NP and electrode materials that can be studied are limited, as the electrode needs to be inert while the NP needs to catalyze the redox reaction of interest.

Particle coulometry is an alternate technique to detect individual NPs that is not limited by NP and electrode materials. Anodic particle coulometry detects NPs in solution *via* their direct oxidation during stochastic collision events at a potentiostated electrode and was originally developed to study single metal NPs in aqueous solution.[21] The technique has been further adapted and applied to size impacting organic[22] and metal oxide[23] NPs and termed cathodic particle coulometry, as these NPs are reduced upon contact with an electrode. Particle coulometry techniques can provide

* Address correspondence to richard.compton@chem.ox.ac.uk.

Received for review May 14, 2014 and accepted June 22, 2014.

Published online June 23, 2014
10.1021/nn502634n

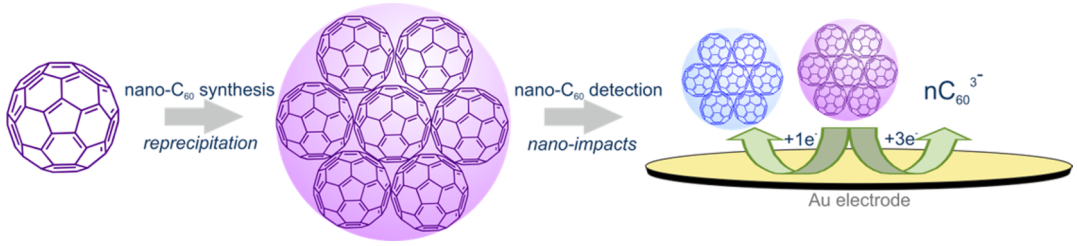

Figure 1. Schematic for the synthesis and electrochemical detection of impacting nano-C_{60} particles at a gold microelectrode where nano-C_{60} is reduced upon collision *via* the transfer of one (represented by the color change from purple to blue) or three electrons, resulting in dissolution of the generated C_{60}^{3-} anions.

the user with information regarding NP size,[21] concentration,[24] stability,[25] and electron transfer kinetics.[26] Importantly in the present work the particle coulometry method not only provides an analytical methodology but also allows direct investigation of the morphology dependency of the redox properties of the C_{60}.

Herein cathodic particle coulometry is used to electrochemically size individual nano-C_{60} particles impacting upon a gold electrode, and it is shown for the first time that this *coulometric* NP sizing technique can be employed not only for the detection of carbonaceous NPs but also in non-aqueous conditions. The morphological influence of transitioning from a molecular microcrystal ensemble to a nanoparticle ensemble to isolated NPs on the electrochemical response of C_{60} is also investigated, and contrasts are drawn between single-nanoparticle and nanoparticle ensemble studies.

RESULTS AND DISCUSSION

Nano-C_{60} particles were synthesized *via* the reprecipitation method,[27] and DLS was used to gain a size distribution for the NP radius, which had a maximum of 16 nm (Figure 1), a size that was confirmed with SEM (19 ± 4 nm).

The electrochemistry of *molecular* C_{60} was investigated prior to the electrochemical characterization of the synthesized nano-C_{60} particles. This approach was chosen as the electrochemical response of molecular C_{60} films has been previously explored in the literature.[28−30] Therefore, the voltammetry of these well-studied molecular C_{60} films provides a useful comparison for the electrochemistry of the synthesized *nanoparticulate* nano-C_{60}. Figure 3a shows the voltammetric response of a molecular C_{60} film in 0.1 M NBu_4PF_6/MeCN, where a gold electrode has been modified with 0.15 mM C_{60} in CH_2Cl_2 (20 μL) as in the work of Tan *et al.*[28] Molecular C_{60} microcrystals form on the electrode surface upon evaporation of the solvent.[28] Ferrocene (2 mM) was added as an internal redox marker for voltammetric experiments, and all potentials are referenced to the ferrocene/ferrocenium redox couple (Fc/Fc^+). Cathodic waves were observed for the first three electron reductions of the molecular C_{60} microcrystals at −1.21, −1.43 and −1.90 V *vs* Fc/Fc^+. The large potential separation between the cathodic

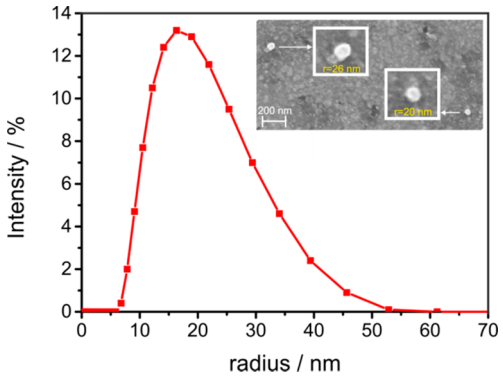

Figure 2. Size distribution for the synthesized stock suspension of nano-C_{60} particles (0.1 mM nano-C_{60} particles in 10% NMP/90% MeCN) measured *via* DLS and SEM image (shown inset) of the same nano-C_{60} stock suspension.

and corresponding anodic peaks observed for the molecular C_{60} microcrystal ensemble has been explained by structural reorganization on the electrode surface to accommodate cation insertion.[29,30] As reported by Jehoulet *et al.*, scanning the potential over the third reduction resulted in the first and second reoxidation waves being significantly altered.[30] This observed change suggests that C_{60}^{3-} is soluble, and hence dissolution of the C_{60} microcrystals occurs after the third electron transfer.[30,31] Dissolution of the third reduction product of the molecular C_{60} microcrystals was confirmed by holding the potential past the third reduction wave for 20 s and then scanning backward, revealing the loss of all reoxidation peaks (SI, Figure S1a).

Having observed the same voltammetric response for a C_{60} microcrystal film as reported in the literature,[28] electrochemical characterization was performed on an ensemble of the nano-C_{60} particles sized in Figure 2. A gold electrode was modified by drop-casting 20 μL of the nano-C_{60} stock suspension (nano-C_{60} as-synthesized in the absence of electrolyte), and cyclic voltammetry was performed in 2 mM Fc/0.1 M NBu_4PF_6/MeCN (Figure 3b). Three reduction waves were observed at −1.09, −1.51 and −2.06 V *vs* Fc/Fc^+. The redox response was found to be markedly different from that of the molecular C_{60} microcystal film. In contrast to the large separation between cathodic and anodic peaks

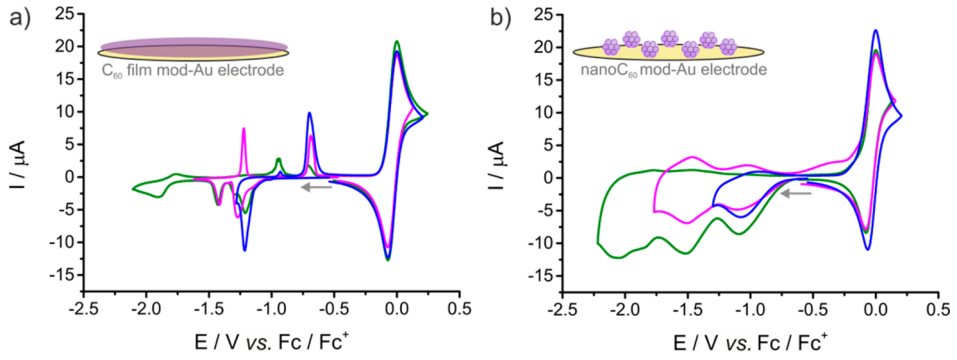

Figure 3. Voltammetric profiles for a Au macroelectrode (r = 0.8 mm) modified with (a) a 20 μL solution of 0.15 mM C_{60} in CH_2Cl_2 and (b) a 20 μL suspension of 0.1 mM nano-C_{60} particles in 10% NMP/90% MeCN to observe the one (blue line), two (pink line), and three (green line) electron reductions of the C_{60} ensembles. All measurements were performed in MeCN (2 mM $Fe(C_5H_5)_2$, 0.1 M NBu_4PF_6) at a scan rate of 100 mV s^{-1}. The redox couple observed at ~0 V is Fc/Fc^+. Arrows represent scan direction.

for the C_{60} microcrystal ensemble, the nano-C_{60}-modified electrode exhibited a much smaller peak-to-peak splitting reflecting voltammetry reported for molecular C_{60}[3] and C_{60} Langmuir–Blodgett films.[30] This difference in electrochemical response demonstrates that a change in the morphology of C_{60} on the electrode surface markedly affects electron transfer. The only similarity between the responses at the microcrystal and nano-C_{60} ensembles is that the third electron reduction of nano-C_{60} is also irreversible, as evidenced by the absence of oxidative features in the reverse scan. The dissolution of nano-C_{60} on the third electron reduction was confirmed *via* the same potential holding method used for the microensemble study above (SI, Figure S1b). A scan rate study of the three-electron reduction of nano-C_{60} (SI, Figure S2) demonstrated that it is the dissolution of the generated C_{60}^{3-} anions as opposed to the electron transfer that is the irreversible step in this third electron reduction, as the proportion of material being reoxidized back onto the electrode surface following the transfer of three electrons increases with increasing scan rate.

Having investigated the change in C_{60} electrochemistry when transitioning from a molecular C_{60} microcrystal ensemble to a nanoparticulate nano-C_{60} ensemble, cathodic particle coulometry was subsequently employed to study the electrochemistry of nano-C_{60} nanoparticles at the single-nanoparticle scale. Cathodic particle coulometry detects and sizes *individual* particles in solution. An aliquot of nano-C_{60} was added to a thoroughly degassed solution of 0.1 M NBu_4PF_6 in MeCN, resulting in a nano-C_{60} concentration of 116 pM before a gold microelectrode (r = 5 μm) suspended in solution was potentiostated to −1.27 V *vs* Fc/Fc^+. This chosen potential corresponds to the one-electron reduction of nano-C_{60} as inferred from Figure 3b. Figure 4 shows the reductive spikes that were observed in the 5 s chronoamperometric scans measured post-addition of nano-C_{60} particles (Figure 4, blue line). Note that no impact spikes were observed in

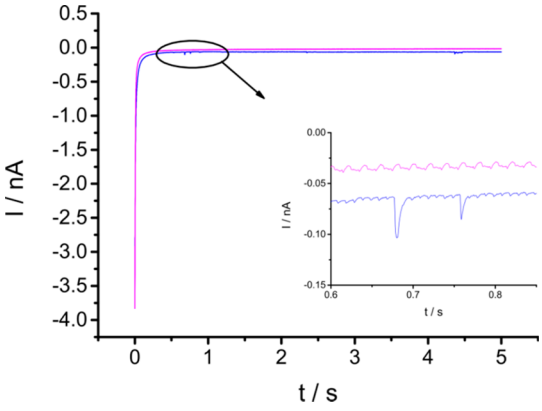

Figure 4. Five second chronoamperogram for a gold microelectrode (r = 5 μm) immersed in a 0.1 M NBu_4PF_6/MeCN solution containing 116 pM nano-C_{60} particles measured at E = −1.27 V *vs* Fc/Fc^+ (blue line) and E = −0.655 V *vs* Fc/Fc^+ (pink line).

solution pre-addition of nano-C_{60}. Each of the reductive spikes observed results from the charge transfer upon a collision between nano-C_{60}, moving *via* Brownian motion in solution, and the gold microelectrode. Increasing the electrode potential to one at which the reduction of nano-C_{60} does not occur (−0.655 V *vs* Fc/Fc^+) caused the observed spikes to disappear (Figure 4, pink line).

A total of 481 impact spikes were recorded for the one-electron reduction of impacting nano-C_{60} (E = −1.27 V *vs* Fc/Fc^+), and the area under each current–time spike was integrated to give the charge for the reduction of each impacting NP. The charge distribution for the impact events recorded where one electron is exchanged is shown in Figure 5a, and the mean charge of the spikes observed was −0.102 ± 0.004 pC (where the error of the mean charge is the standard error of the mean given by SD/$\sqrt{n}$ where SD is the standard deviation and n is the sample number, in this case the number of spikes). If the whole NP is reduced upon impact and a spherical particle shape is assumed, the Faradaic charge measured for the

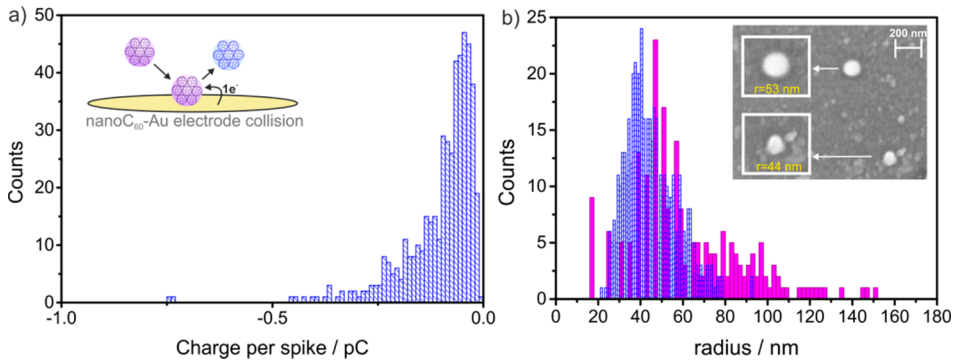

Figure 5. (a) Charge distribution with a bin size of 0.01 pC for the one-electron reduction of nano-C_{60} (116 pM) impacting a gold microelectrode (r = 5 μm) in MeCN (0.1 M NBu_4PF_6) (b) Size distribution with a bin size of 1 nm for the one-electron reduction of nano-C_{60} (116 pM) impacting a Au electrode (r = 5 μm) in MeCN (0.1 M NBu_4PF_6) (blue) overlaid with the size distribution determined by SEM imaging of nano-C_{60} particles dispersed in 0.1 M NBu_4PF_6/MeCN (pink, bin size = 2 nm) and SEM image shown in inset.

observed NP−electrode collisions can be reinterpreted to determine the radius of each impacting NP *via*

$$r = \sqrt[3]{\frac{3MQ}{4\pi Fz\rho}} \quad (1)$$

where M is the molecular mass of C_{60} in kg mol^{-1}, Q is the charge measured in coulombs (C), F is Faraday's constant in C mol^{-1}, z is the number of electrons transferred, and ρ is the density of C_{60} measured in kg m^{-3}.

The NP size distribution determined using eq 1 is shown in Figure 5b (blue), and the mean radius was 45 ± 12 nm (where the error is given by the SD), significantly larger than the size of nano-C_{60} in the synthesized stock NP suspension measured using DLS and SEM (∼20 nm radius). It is well known that nano-C_{60} particles are prone to aggregation upon the addition of salt;[7,32] therefore we suggest that the larger NP size determined from the cathodic particle coulometry experiment is due to the aggregation of nano-C_{60} NPs when dispersed in a 0.1 M NBu_4PF_6/MeCN solution. A size distribution of nano-C_{60} in the presence of the electrolyte could not be measured *via* DLS, as the aggregating particles resulted in a very high polydispersity within the sample. SEM analysis of nano-C_{60} particles in 0.1 M NBu_4PF_6/MeCN was performed to determine if the NPs aggregate in the presence of the electrolyte used for the cathodic particle coulometry experiments. The measurements were carried out by drop-casting a sample of the nano-C_{60} particles suspended in electrolyte on a SEM sample holder that had been modified with a transmission electron microscopy grid in order to minimize NP aggregation during sample preparation. SEM analysis showed that the NP size increased upon nano-C_{60} dispersion in 0.1 M NBu_4PF_6/MeCN, and relatively good agreement was found between the nano-C_{60} size distributions measured *via* SEM and cathodic particle coulometry in the presence of electrolyte (Figure 5b). There is an increased occurrence of larger particles (radius ∼80−150 nm) in the SEM-determined NP size distribution, which could be due to the aggregation of nano-C_{60} during preparation of the SEM sample despite steps having been taken to minimize this effect. Another possible explanation for the discrepancy between the cathodic particle coulometry and SEM-determined size distributions is that slower diffusion coefficients of larger NPs will result in a reduced collision probability during impact experiments, and therefore larger NPs are less likely to be measured *via* particle coulometry; this phenomenon has been investigated using silver NPs by Lees *et al.*[33]

The accurate sizing of nano-C_{60} from impact events observed when the electrode is held at the potential for a one-electron reduction, as determined from the voltammetric response of the nano-C_{60} ensemble (Figure 3b), demonstrates that there is no change in the potential at which this first electron transfer occurs when changing from an NP ensemble to individual NPs. In contrast, changes are observed for the third electron reduction of nano-C_{60} when the electrochemical response of the NP ensemble is compared to single collision events. It is known that peak potentials can shift by up to hundreds of millivolts when the voltammetry of an NP ensemble with strongly overlapping NP diffusion layers is compared to a case where the NPs are isolated and therefore diffusionally independent.[34] The voltammetric response shown in Figure 3b for the NP ensemble, where the NP diffusion layers will be overlapping, demonstrates that the second electron reduction of nano-C_{60} is a reversible process, while the third cathodic wave observed is irreversible and results in the formation of the soluble C_{60}^{3-} product that will diffuse away from the electrode.[30,31] For single collision events, a shift in potential occurs only for the irreversible third electron transfer, as the ease of nano-C_{60} dissolution at the isolated NP scale lowers the potential required for the third electron reduction and results from the strong divergent diffusion of products away from individual NPs as compared to the semi-infinite, planar diffusion seen for high coverage layers on electrode surfaces. Figure 6a

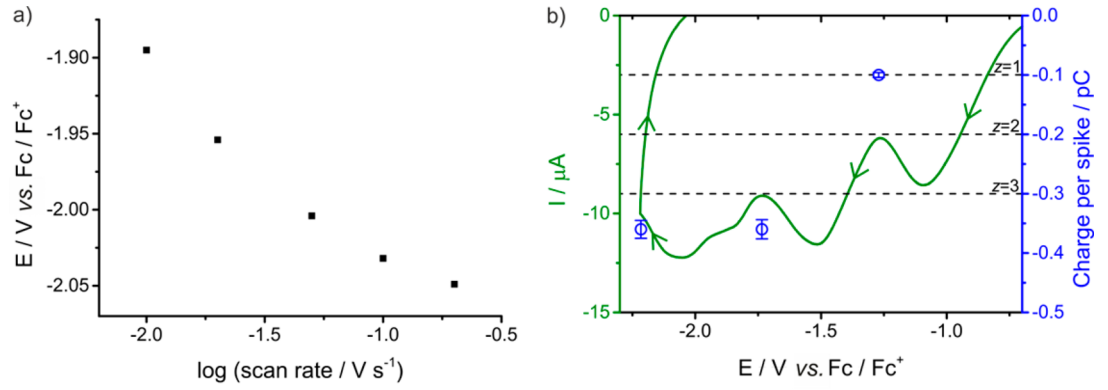

Figure 6. (a) Plot of potential for the third electron reduction peak of nano-C_{60} against log(scan rate) for a 20 μL nano-C_{60} modified Au macroelectrode (r = 0.8 mm) in a solution of 2 mM $Fe(C_5H_5)_2$, 0.1 M NBu_4PF_6 in MeCN. (b) Voltammogram of a Au macroelectrode (r = 0.8 mm) modified with 20 μL of 0.1 mM nano-C_{60} particles scanned in MeCN (2 mM $Fe(C_5H_5)_2$, 0.1 M NBu_4PF_6) at a scan rate of 100 mV s^{-1} (green line) overlaid with a plot of potential against the mean charge transfer per impacting nano-C_{60} particle (blue symbols) where the error bars are determined by the standard error of the mean.

demonstrates that as the scan rate for nano-C_{60} ensemble studies is decreased, the third electron reduction of nano-C_{60} becomes more favorable and is observed at increasingly positive potentials (voltammograms are shown in the SI, Figure S2).

Cathodic particle coulometry experiments performed at potentials corresponding *nominally* to the second ($E = -1.74$ V *vs* Fc/Fc^+) and third ($E = -2.22$ V *vs* Fc/Fc^+) electron transfers as inferred from the ensemble studies (Figure 3b) show a shift in potential at the *single*-NP scale. For impact events measured at the former potential the mean charge was -0.360 ± 0.016 pC; this charge transfer is identical to the mean charge for current−time spikes observed for nano-C_{60} particles undergoing a three-electron reduction upon collision (-0.360 ± 0.015 pC). This similarity in charge suggests that a three-electron reduction is observed for impacting NPs held at the potentials where the NP ensemble shows a two- and three-electron reduction of nano-C_{60} should be occurring. This change in redox behavior is due to the study of *isolated* NPs *via* particle coulometry as opposed to an NP ensemble.

Figure 6b shows that if the charge transfer for a one-electron reduction of a single impacting nano-C_{60} particle is fixed at -0.10 pC, the value observed for the cathodic particle coulometry experiment performed at $E = -1.27$ V *vs* Fc/Fc^+, we can make the assumption that a three-electron transfer occurs for cathodic particle coulometry experiments at both -1.74 and -2.22 V *vs* Fc/Fc^+, as the mean charge measured at these potentials (-0.36 pC) is approximately three times the value of that for a one-electron reduction at the single NP scale. This is further supported by re-interpretation of the charge transfer data measured at $E = -1.74$ V *vs* Fc/Fc^+ in terms of radius *via* eq 1 with the assumption $z = 3$, giving a mean radius of 44 ± 17 nm (SI, Figure S4b), in good agreement with mean radius values determined for the other two potentials studied ($r = 45 \pm 12$ nm at $E = -1.27$ V *vs* Fc/Fc^+; $r = 44 \pm 17$ nm at $E = -2.22$ V *vs* Fc/Fc^+). Hence for single-NP studies, the third electron reduction of nano-C_{60} occurs at an earlier potential than that observed for the NP ensemble, demonstrating that the electrochemical response of nano-C_{60} can differ when a NP ensemble is examined as opposed to an isolated NP.

CONCLUSIONS

In summary, we have reported the electrochemical detection and sizing of individual nano-C_{60} nanoparticles, demonstrating for the first time that NP-electrode impact studies can be performed in non-aqueous systems and cathodic particle coulometry can be applied to size carbonaceous nanoparticles. It is shown that a potential shift of the third electron transfer process occurs at the single-NP scale when compared to the peak potential at which this process is observed in the voltammetry of a nano-C_{60} ensemble. Thus, the electrochemical response is altered when changing from an ensemble of nano-C_{60} NPs present on an electrode surface to an isolated NP scenario. Another factor that was found to strongly influence C_{60} electron transfer is the morphology of C_{60} on the electrode surface with significant changes in the voltammetric response observed between micro- and nano-C_{60} ensembles.

METHODS

Nano-C_{60} particles were synthesized using the reprecipitation method.[27] The method used here is based on the work by Zhang *et al.*;[35] however the nanoparticles were reprecipitated in acetonitrile rather than water as in the nano-C_{60} synthesis reported by Alargova *et al.*[36] First, 17.2 mg of C_{60} (99.5% pure, SES Research, TX, USA) was dissolved in 20 mL of *N*-methyl-2-pyrrolidone (NMP, Sigma-Aldrich) by stirring in the dark for 24 h. The C_{60}-containing NMP solution was then added dropwise to 200 mL of stirring MeCN (Sigma-Aldrich) at a speed of

0.9 mL min^{-1} before continuing to stir for 30 min in the dark. The NP solution was passed through a 0.2 μm filter (Whatman International Ltd., Kent, UK), resulting in a transparent orange solution of 0.1 mM nano-C_{60} NPs (radius ~16 nm according to DLS) in 10% NMP/90% MeCN. This concentration does not take into account the loss of material during filtration. DLS measurements were performed using a Malvern Zetasizer Nano ZS, and a LEO Gemini 1530 (Zeiss, Oberkochen, Germany) was employed for SEM imaging. An SEM holder that had been modified with a transmission electron microscopy grid was used for SEM experiments in order to minimize nano-C_{60} aggregation during sample preparation.

All electrochemical studies were carried out using a μAutolab II (Metrohm-Autolab BV, Utrecht, Netherlands) at 25 $\pm$ 0.2 °C in an oxygen-free 0.1 M NBu_4PF_6/MeCN solution using a three-electrode setup with a carbon rod counter electrode, a silver wire pseudo-reference electrode, and either a macro (r = 0.8 mm) or micro (r = 5 μm) gold working electrode (CH Instruments, Texas, USA). Working electrodes were polished with alumina powder (1, 0.3, and 0.05 μm) prior to each experiment. Ferrocene (2 mM) was added to the electrolyte solution to act as an internal redox marker for voltammetric measurements. To prepare a solution of 0.15 mM C_{60} in CH_2Cl_2, the solution was stirred in the dark for 24 h. Modification of the gold macroelectrode was performed by drop-casting 4 $\times$ 5 μL layers of C_{60} solution/nano-C_{60} suspension before drying at 35 $\pm$ 0.2 °C. Due to the low surface tension of the solvents used, solution run-off onto the insulator surrounding the electrode surface could not be prevented, and therefore quantification of the amount of nano-C_{60} immobilized on the electrode was not possible. Cathodic particle coulometry experiments were performed within a double faraday cage to reduce noise. All glassware was cleaned with aqua regia (75% HCl/25% HNO_3) and oven-dried to remove any traces of water. The nitrogen flow used to degas solutions was purged with acetonitrile that had been dried with molecular sieves to ensure no water was introduced to the system.

ImageJ (Version 1.38) was used to analyze the NP size determined *via* SEM, while SignalCounter developed by Dr. Dario Omanović at the Ruđer Bošković Institute in Zagreb, Croatia, was employed for the analysis of spikes observed in cathodic particle coulometry experiments.

Conflict of Interest: The authors declare no competing financial interest.

Acknowledgment. This research is supported by the European Research Council under the European Union's Seventh Framework Programme (FP/2007-2013)/ERC Grant Agreement No. 320403 (C.B.-M.), a Marie Curie Intra European Fellowship within the 7th European Community Framework Programme (K.T.), the Leverhulme Trust (Grant No. F/08 788/J), and the Armourers and Brasiers' Company (E.J.E.S.). We thank K. Hennig (IFW Dresden, Germany) and K. Jurkschat (University of Oxford, UK) for assistance with SEM and DLS measurements, respectively.

Supporting Information Available: Voltammetric profiles measured post 20 s chronamperograms for the first three electron reductions of microcrystalline C_{60} and nano-C_{60}, scan rate study of a nano-C_{60}-modified Au macroelectrode, impact spikes observed for cathodic particle coulometry experiments at E = −1.74 V and −2.22 V *vs* Fc/Fc^+, charge and size distributions determined from these observed impact spikes. This material is available free of charge *via* the Internet at http://pubs.acs.org.

REFERENCES AND NOTES

1. Kroto, H. W.; Heath, J. R.; O'Brien, S. C.; Curl, R. F.; Smalley, R. E. C_{60}: Buckminsterfullerene. *Nature* **1985**, *318*, 162–163.
2. Jehoulet, C.; Bard, A. J.; Wudl, F. Electrochemical Reduction and Oxidation of C_{60} Films. *J. Am. Chem. Soc.* **1991**, *113*, 5456–5457.
3. Xie, Q. S.; Perezcordero, E.; Echegoyen, L. Electrochemical Detection of C_{60}^{6-} and C_{70}^{6-}: Enhanced Stability of Fullerides in Solution. *J. Am. Chem. Soc.* **1992**, *114*, 3978–3980.
4. Eng, A. Y. S.; Pumera, M. Direct Voltammetry of Colloidal Graphene Oxides. *Electrochem. Commun.* **2014**, *43*, 87–90.
5. Barazzouk, S.; Hotchandani, S.; Kamat, P. V. Unusual Electrocatalytic Behavior of Ferrocene Bound Fullerene Cluster Films. *J. Mater. Chem.* **2002**, *12*, 2021–2025.
6. Kamat, P. V.; Barazzouk, S.; Thomas, K. G.; Hotchandani, S. Electrodeposition of C_{60} Cluster Aggregates on Nanostructured SnO_2 Films for Enhanced Photocurrent Generation. *J. Phys. Chem. B* **2000**, *104*, 4014–4017.
7. Brant, J.; Lecoanet, H.; Hotze, M.; Wiesner, M. Comparison of Electrokinetic Properties of Colloidal Fullerenes (*n*-C_{60}) Formed Using Two Procedures. *Environ. Sci. Technol.* **2005**, *39*, 6343–6351.
8. Zhou, Z. G.; Lenk, R.; Dellinger, A.; MacFarland, D.; Kumar, K.; Wilson, S. R.; Kepley, C. L. Fullerene Nanomaterials Potentiate Hair Growth. *Nanomedicine* **2009**, *5*, 202–207.
9. Li, G.; Shrotriya, V.; Huang, J. S.; Yao, Y.; Moriarty, T.; Emery, K.; Yang, Y. High-Efficiency Solution Processable Polymer Photovoltaic Cells by Self-Organization of Polymer Blends. *Nat. Mater.* **2005**, *4*, 864–868.
10. Buseck, P. R.; Tsipursky, S. J.; Hettich, R. Fullerenes from the Geological Environment. *Science* **1992**, *257*, 215–217.
11. Daly, T. K.; Buseck, P. R.; Williams, P.; Lewis, C. F. Fullerenes from a Fulgurite. *Science* **1993**, *259*, 1599–1601.
12. Lyon, D. Y.; Adams, L. K.; Falkner, J. C.; Alvarez, P. J. J. Antibacterial Activity of Fullerene Water Suspensions: Effects of Preparation Method and Particle Size. *Environ. Sci. Technol.* **2006**, *40*, 4360–4366.
13. Sayes, C. M.; Fortner, J. D.; Guo, W.; Lyon, D.; Boyd, A. M.; Ausman, K. D.; Tao, Y. J.; Sitharaman, B.; Wilson, L. J.; Hughes, J. B.; *et al*. The Differential Cytotoxicity of Water-Soluble Fullerenes. *Nano Lett.* **2004**, *4*, 1881–1887.
14. Xiao, X. Y.; Bard, A. J. Observing Single Nanoparticle Collisions at an Ultramicroelectrode by Electrocatalytic Amplification. *J. Am. Chem. Soc.* **2007**, *129*, 9610–9612.
15. Xiao, X. Y.; Fan, F. R. F.; Zhou, J. P.; Bard, A. J. Current Transients in Single Nanoparticle Collision Events. *J. Am. Chem. Soc.* **2008**, *130*, 16669–16677.
16. Kwon, S. J.; Fan, F. R. F.; Bard, A. J. Observing Iridium Oxide (IrOx) Single Nanoparticle Collisions at Ultramicroelectrodes. *J. Am. Chem. Soc.* **2010**, *132*, 13165–13167.
17. Dasari, R.; Robinson, D. A.; Stevenson, K. J. Ultrasensitive Electroanalytical Tool for Detecting, Sizing, and Evaluating the Catalytic Activity of Platinum Nanoparticles. *J. Am. Chem. Soc.* **2013**, *135*, 570–573.
18. Dasari, R.; Walther, B.; Robinson, D. A.; Stevenson, K. J. Influence of the Redox Indicator Reaction on Single-Nanoparticle Collisions at Mercury- and Bismuth-Modified Pt Ultramicroelectrodes. *Langmuir* **2013**, *29*, 15100–15106.
19. Dasari, R.; Tai, K.; Robinson, D. A.; Stevenson, K. J. Electrochemical Monitoring of Single Nanoparticle Collisions at Mercury-Modified Platinum Ultramicroelectrodes. *ACS Nano* **2014**, *8*, 4539–4546.
20. Park, J. H.; Thorgaard, S. N.; Zhang, B.; Bard, A. J. Single Particle Detection by Area Amplification: Single Wall Carbon Nanotube Attachment to a Nanoelectrode. *J. Am. Chem. Soc.* **2013**, *135*, 5258–5261.
21. Zhou, Y. G.; Rees, N. V.; Compton, R. G. The Electrochemical Detection and Characterization of Silver Nanoparticles in Aqueous Solution. *Angew. Chem., Int. Ed.* **2011**, *50*, 4219–4221.
22. Cheng, W.; Zhou, X. F.; Compton, R. G. Electrochemical Sizing of Organic Nanoparticles. *Angew. Chem., Int. Ed.* **2013**, *52*, 12980–12982.
23. Tschulik, K.; Haddou, B.; Omanović, D.; Rees, N. V.; Compton, R. G. Coulometric Sizing of Nanoparticles: Cathodic and Anodic Impact Experiments Open Two Independent Routes to Electrochemical Sizing of Fe_3O_4 Nanoparticles. *Nano Res.* **2013**, *6*, 836–841.
24. Stuart, E. J. E.; Zhou, Y. G.; Rees, N. V.; Compton, R. G. Determining Unknown Concentrations of Nanoparticles: The Particle-Impact Electrochemistry of Nickel and Silver. *RSC Adv.* **2012**, *2*, 6879–6884.
25. Qiu, D. F.; Wang, S.; Zheng, Y. Q.; Deng, Z. X. One at a Time: Counting Single-Nanoparticle/Electrode Collisions for

Accurate Particle Sizing by Overcoming the Instability of Gold Nanoparticles under Electrolytic Conditions. *Nanotechnology* **2013**, *24*, 505707.
26. Haddou, B.; Rees, N. V.; Compton, R. G. Nanoparticle-Electrode Impacts: The Oxidation of Copper Nanoparticles Has Slow Kinetics. *Phys. Chem. Chem. Phys.* **2012**, *14*, 13612–13617.
27. Kasai, H.; Nalwa, H. S.; Oikawa, H.; Okada, S.; Matsuda, H.; Minami, N.; Kakuta, A.; Ono, K.; Mukoh, A.; Nakanishi, H. A Novel Preparation Method of Organic Microcrystals. *Jpn. J. Appl. Phys., Part 2* **1992**, *31*, L1132–L1134.
28. Tan, W. T.; Lim, E. B.; Bond, A. M. Voltammetric Studies on Microcrystalline C_{60} Adhered to an Electrode Surface by Solvent Casting and Mechanical Transfer Methods. *J. Solid State Electrochem.* **2003**, *7*, 134–140.
29. Suarez, M. F.; Marken, F.; Compton, R. G.; Bond, A. M.; Miao, W. J.; Raston, C. L. Evidence for Nucleation-Growth, Redistribution, and Dissolution Mechanisms during the Course of Redox Cycling Experiments on the C_{60}/NBu_4C_{60} Solid-State Redox System: Voltammetric, SEM, and *in Situ* AFM Studies. *J. Phys. Chem. B* **1999**, *103*, 5637–5644.
30. Jehoulet, C.; Obeng, Y. S.; Kim, Y. T.; Zhou, F. M.; Bard, A. J. Electrochemistry and Langmuir Trough Studies of C_{60} and C_{70} Films. *J. Am. Chem. Soc.* **1992**, *114*, 4237–4247.
31. Bond, A. M.; Miao, W. J.; Raston, C. L. Identification of Processes that Occur after Reduction and Dissolution of C_{60} Adhered to Gold, Glassy Carbon, and Platinum Electrodes Placed in Acetonitrile (Electrolyte) Solution. *J. Phys. Chem. B* **2000**, *104*, 2320–2329.
32. Deguchi, S.; Alargova, R. G.; Tsujii, K. Stable Dispersions of Fullerenes, C_{60} and C_{70}, in Water. Preparation and Characterization. *Langmuir* **2001**, *17*, 6013–6017.
33. Lees, J. C.; Ellison, J.; Batchelor-McAuley, C.; Tschulik, K.; Damm, C.; Omanović, D.; Compton, R. G. Nanoparticle Impacts Show High-Ionic-Strength Citrate Avoids Aggregation of Silver Nanoparticles. *ChemPhysChem* **2013**, *14*, 3895–3897.
34. Toh, H. S.; Batchelor-McAuley, C.; Tschulik, K.; Uhlemann, M.; Crossley, A.; Compton, R. G. The Anodic Stripping Voltammetry of Nanoparticles: Electrochemical Evidence for the Surface Agglomeration of Silver Nanoparticles. *Nanoscale* **2013**, *5*, 4884–4893.
35. Zhang, S. A.; Sakai, R.; Abe, T.; Iyoda, T.; Norimatsu, T.; Nagai, K. Photoelectrochemical and Photocatalytic Properties of Biphasic Organic p- and n-Type Semiconductor Nanoparticles Fabricated by a Reprecipitation Process. *ACS Appl. Mater. Interfaces* **2011**, *3*, 1902–1909.
36. Alargova, R. G.; Deguchi, S.; Tsujii, K. Stable Colloidal Dispersions of Fullerenes in Polar Organic Solvents. *J. Am. Chem. Soc.* **2001**, *123*, 10460–10467.